Article

Three-Membered Ring or Open Chain Molecule – (FC)FSiONMe a Model for the -Effect in Silicon Chemistry

Norbert W. Mitzel, Krunoslav Vojinovi, Roland Frhlich, Thomas Foerster, Heather E. Robertson, Konstantin B. Borisenko, and David W. H. Rankin

J. Am. Chem. Soc., **2005**, 127 (39), 13705-13713• DOI: 10.1021/ja052865o • Publication Date (Web): 08 September 2005

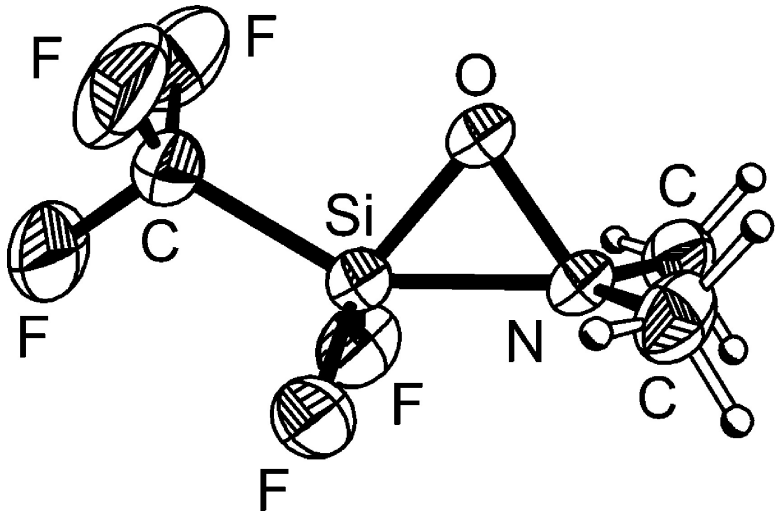

More About This Article

Additional resources and features associated with this article are available within the HTML version:

- Supporting Information
- Links to the 2 articles that cite this article, as of the time of this article download
- Access to high resolution figures
- Links to articles and content related to this article
- Copyright permission to reproduce figures and/or text from this article

View the Full Text HTML

J|A|C|S
ARTICLES
Published on Web 09/08/2005

Three-Membered Ring or Open Chain Molecule − $(F_3C)F_2SiONMe_2$ a Model for the α-Effect in Silicon Chemistry

Norbert W. Mitzel,*,† Krunoslav Vojinović,† Roland Fröhlich,‡ Thomas Foerster,§ Heather E. Robertson,§ Konstantin B. Borisenko,§ and David W. H. Rankin§

Contribution from the Institut für Anorganische und Analytische Chemie, Westfälische Wilhelms-Universität Münster, Corrensstr. 30, D-48149 Münster, Germany, Organisch-chemisches Institut, Westfälische Wilhelms-Universität Münster, Corrensstr. 40, D-48149 Münster, Germany, and School of Chemistry, University of Edinburgh, West Mains Road, Edinburgh EH9 3JJ, UK

Received May 2, 2005; E-mail: mitzel@uni-muenster.de

Abstract: $(F_3C)F_2SiONMe_2$ was prepared from $LiONMe_2$ and F_3CSiF_3. It was characterized by gas IR and multinuclear solution NMR spectroscopy and by mass spectrometry. Its structure was elucidated by single crystal X-ray crystallography and by gas electron diffraction. (It exists as a conformer mixture.) Important findings were extremely acute SiON angles [solid 74.1(1)°, gas anti 84.4(32)° and gauche 87.8(20)°] and short Si···N distances [solid 1.904(2) Å]. The bending potential of the SiON unit was calculated at the MP2/6-311++G(3df,2dp) level of theory and appears very flat and highly asymmetric. The calculated atomic charges (NPA) are counterintuitive to the expected behavior for a classical Si−N dative bond, as upon formation of the Si···N bond electron density is transferred mainly from oxygen to nitrogen, while the silicon charge is almost unaffected. Despite the molecular topology of a three-membered ring, the topology of the electron density shows neither a bond critical point between Si and N atoms nor a ring critical point, but the electron density and Laplacian values are related to other hypercoordinate Si compounds. The electronic properties of $(F_3C)F_2SiONMe_2$ were compared to those of the adduct $(F_3C)F_2(MeO)Si{-}NMe_3$, whose properties and structure were also calculated. The charge distribution and Laplacian values along the Si−N vectors in both molecules are similar but not equivalent. $(F_3C)F_2SiONMe_2$ contains thus a nonclassical Si···N bond, and its properties can be regarded as a new model for the explanation of the old postulate of an α-effect in silicon chemistry, explaining the behavior of compounds with geminal Si and N atoms.

Introduction

The nature of interactions between geminal donor and acceptor atoms in main-group systems has been a matter of debate for more than 40 years. The early picture of a classical dative bond between a silicon atom and a geminal donor center (Scheme 1) was introduced by Kostyanovski[1] in order to rationalize the reactivity and properties of geminal systems.[2]

Data from various spectroscopic techniques were used to confirm the above model[3] for a range of different classes of compounds (Z = C, N, O ...). This picture was used to develop

Scheme 1

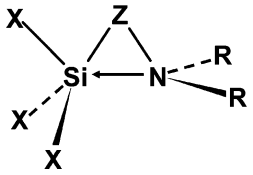

the industrially important and highly reactive class of α-functionalized silanes, including aminomethylsilanes, isocyanatomethylsilanes, and alkoxycarbosilanes.[4] However, a series of recent investigations on aminomethylsilanes (SiCN units)[5] and methoxymethylsilanes (SiCO units)[6] did not provide structural evidence for the existence of such an effect, whereas in hydrazinosilanes (SiNN units)[7] and hydroxylaminosilanes (SiON units)[8] relatively strong interactions between the geminal Si and

† Institut für Anorganische und Analytische Chemie, Westfälische Wilhelms-Universität Münster.

‡ Organisch-chemisches Institut, Westfälische Wilhelms-Universität Münster.

§ University of Edinburgh.

(1) (a) Kostyanovskii, R. G.; Prokov'ev, A. K. *Dokl. Akad. Nauk SSSR* **1965**, *164*, 1054−1057. (b) Kharpov, V. V.; Gol'danskii, V. I.; Prokov'ev, A. K.; Kostyanovskii, R. G. *Zh. Obshch. Khim.* **1967**, *37*, 3.

(2) (a) Wilkinson, G.; Stone, F. G. A.; Abel E. W. *Comprehenshive Organometallic Chemistry*, 1st ed.; Pergamon Press: Oxford, 1982, Vol. 2, p 412. (b) Voronkov, M. G.; Kashik, T. V.; Lukevits, E. Y.; Deriglazova, E. S.; Pestunovich, A. E.; Moskovich, R. Y. *Zh. Obshch. Khim.* **1974**, *44*, 778. (c) Khorshev, S. Y.; Egorochkin, A. N.; Sevast'yanova, E. I.; Ostasheva, N. S.; Kuz'min, O. V. *Zh. Obshch. Khim.* **1976**, *46*, 1795. (d) Feshin, V. P.; Voronkov, M. G. *J. Mol. Struct.* **1982**, *83*, 317.

(3) Egorochkin, N.; Skobeleva, S. E.; Sevast'yanova, E. I.; Kosolapova, I. G.; Sheludyakov, V. D.; Rodionov, E. S.; Kirilin, A. D. *Zh. Obsh. Khim.* **1976**, *46*, 1795.

(4) (a) Bauer, A.; Kammel, T.; Pachaly, B.; Schäfer, O.; Schindler, W.; Stanjek, V.; Weis, J. In Organosilicon Chemistry V; Auner, N.; Weis, J., Eds.; Wiley-VCH: Weinheim, 2003; p 527. (b) One step ahead − organofunctional silanes from Wacker, Brochure of the Wacker company http://www.wacker.com/Internet/webcache/de_DE/BrochureOrder/GENIOSIL-_Brosch_e.pdf. (c) Schindler, W. *Adhäsion* **2004**, *12.04*, 29.

(5) (a) Lazareva, N. F.; Baryshok, V. P.; Voronkov, M. G. *Russ. Chem. Bull.* **1995**, *44*, 374. (b) Mitzel, N. W.; Kiener, C.; Rankin, D. W. H. *Organometallics* **1999**, *18*, 3437. (c) Mitzel, N. W. *Z. Naturforsch.* **2003**, *58 b*, 369.

(6) Mitzel, N. W. *Z. Naturforsch.* **2003**, *58 b*, 759.

N atoms could be detected. Accompanying theoretical investigations have shown the above model to be far too simple to account for the details of the Si···N interaction between the geminal Si and N atoms. The lack of an accumulation of electron density[9] between these atoms and the high dependence of the strength of the interaction on the mutual orientation of the contributing dipoles[10] indicates a predominant contribution of electrostatic or dipole forces.

The stronger such geminal Si···N interactions are the clearer should be an assignment to individual attractive and repulsive contributions. In the search for the maximum Si···N interaction strength we have now synthesized a Si-trifluoromethylated silylhydroxylamine, as CF_3 groups have almost the group electronegativity of F atoms but are not capable of back-bonding toward the silicon center. With a detailed investigation of the bonding situation we will show in this contribution that the interaction between the geminal Si and N atoms cannot be described by models commonly expected to be applicable to this problem.

Experimental Section

Preparation. A solution of *n*-butyllithium (9.6 mL, 1.6 M in hexane, 15 mmol) was added dropwise to a solution of *N*,*N*-dimethylhydroxylamine (0.8 mL, 1.0 g, 16 mmol) in pentane (20 mL) at −50 °C, allowed to warm to ambient temperature and stirred for 1 h. The solvents were removed in vacuo. Dry dimethyl ether (15 mL) was condensed onto the resulting $LiONMe_2$ at −196 °C followed by trifluoro(trifluoromethyl)silane[11] (3.5 g, 23 mmol). The mixture was warmed to −96 °C and then allowed to warm slowly for 4 h to −25 °C while stirring. The volatile components were condensed off and fractionated repeatedly through a series of cold traps held at −50, −90, and −196 °C. 2.1 g of $(F_3C)F_2SiONMe_2$ (11 mmol, 69%) were collected in the −50 °C trap. Mp −43 °C, very sensitive to air and moisture. ^{1}H NMR (d_8-toluene, −30 °C): δ 2.14 (s, CH_3). $^{13}C\{^1H\}$ NMR: δ 48.0 (s, CH_3), 138.0 (m, CF_3). $^{15}N\{^1H\}$ NMR: δ −264.1 (t, $^3J_{NOSiF}$ = 11.9 Hz). ^{19}F NMR: δ −76.8 (d), 11.3 (t, $^3J_{FCSiF}$ = 7.9 Hz). ^{29}Si NMR: δ −116.8 (tq, $^1J_{SiF}$ = 252.5 Hz, $^2J_{SiCF}$ = 64.0 Hz). IR (gas): ν (cm^{-1}) 3009 (w), 2982 (w), 2926 (m), 2892 (m), 2836 (w), 2818 (w), 2807 (w, νCH), 1464 (w), 1248 (w), 1179 (m), 1192 (m), 1132 (vs, νSiF), 1024 (s), 984 (m), 954 (m), 866 (m), 835 (w), 765 (w).

Crystallography. A single crystal of $(F_3C)F_2SiONMe_2$ was grown in situ by establishing a solid−liquid equilibrium in a sealed capillary, selecting a suitable seed crystal while melting the rest, followed by slowly lowering the temperature until the capillary was filled with one single crystal. Diffractometer: Nonius Kappa CCD, Mo Kα radiation, formula $C_3H_6F_5NOSi$, M_w = 195.16 g mol^{-1}, crystal system orthorhombic, space group *Pnma*, a = 8.941(1), b = 10.139(1), c = 8.765(1) Å, V = 794.57(15) Å^3, Z = 4, ρ_{calc} 1.632 g cm^{-3}, $F(000)$ = 392 e, μ = 0.331 mm^{-1}, T = 150(2) K, θ-range 3.07°−28.67°. 1835 measured scattering intensities of which 1036 were independent, R_{int} = 0.0148. 70 refined parameters,[12] R_1 = 0.0387, wR_2 = 0.0981, ρ_{fin} (max/min) 0.0279/−0.257 e Å^{-3}. CCDC-258262 contains the supplementary crystallographic data for this paper. These data can be obtained free of charge via www.ccdc.cam.ac.uk/conts/retrieving.html (or from the Cambridge Crystallographic Data Centre, 12 Union Road, Cambridge CB2 1EZ, UK (fax: (+44)1223-336-033; or deposit@ccdc.cam.ac.uk).

Gas Electron Diffraction. The Edinburgh gas-diffraction apparatus[13] was used to collect data. The sample and nozzle temperatures were held at 243 and 293 K, respectively. An accelerating voltage of ca. 40 kV (electron wavelength ca. 6.0 pm) was used, and the scattering intensities for both compounds were recorded at nozzle-to-film distances of 129.55 and 286.94 mm on Kodak Electron Image film. For calibration and to minimize any systematic errors in wavelength and camera distances, the scattering patterns of benzene were also collected and analyzed in the same way. The electron-scattering patterns were converted into digital form with a scanning program described elsewhere[14] using an Epson scanner. Three diffraction patterns were collected at each nozzle-to-plate distance giving data sets in the ranges (weighting points for off-diagonal weight matrixes in parentheses) 20 to 118 nm^{-1} (40, 102 nm^{-1}) and 80 to 268 nm^{-1} (100, 232 nm^{-1}). Data reduction and least-squares refinements were carried out using standard programs[15] employing the scattering factors of Ross et al.[16] Correlation parameters were 0.4685 and 0.3846, scale factors, 1.6173 and 1.2023, and final R_G values, 0.0392 and 0.0752 for the two data sets, respectively. Further data and scattering intensity curves are provided in the Supporting Information to this paper.

Quantum Chemical Calculations. Geometry optimizations and vibrational frequency calculations were performed at Hartree−Fock (HF), MP2, and DFT levels of theory. Different basis sets of increasing size were employed, namely the standard basis sets 3-21G(d), 6-31G(d), and 6-31G(d,p) as well as the more extended 6-311G(d,p), 6-311+G(d,p), and 6-311++G(3df,2pd) basis sets.[17] All MP2 calculations were carried out with a frozen core.

The electron density distribution, $\rho(r)$, was analyzed using the virial partitioning method of Bader and co-workers.[18] The Laplace concentration $-\nabla^2\rho(r)$ was analyzed to determine regions of charge concentration and depletion. Atomic charges were calculated using the natural atomic orbital (NAO) population analysis.[19] All calculations were performed with the ab initio program GAUSSIAN 98[20] and the electron density analysis package AIM2000.[21]

Results

Synthesis and Characterization. The reaction of the difluorocarbene generator F_3CSiF_3[11] with $LiONMe_2$ in dimethyl ether gave $(F_3C)F_2SiONMe_2$ in 69% yield.

$$F_3CSiF_3 + LiONMe_2 \rightarrow LiF + (F_3C)F_2SiONMe_2$$

$(F_3C)F_2SiONMe_2$ is a volatile liquid, which decomposes rapidly

(7) (a) Mitzel, N. W. *Chem. Eur. J.* **1998**, *4*, 692. (b) Vojinović, K.; McLachlan, L.; Rankin, D. W. H.; Mitzel, N. W. *Chem. Eur. J.* **2004**, *10*, 3033.
(8) (a) Schmatz, S.; Diedrich, F.; Ebker, C.; Klingebiel, U. *Eur. J. Inorg. Chem.* **2002**, 876. (b) Schmatz, S.; Ebker, C.; Labahn, T.; Stoll, H.; Klingebiel, U. *Organometallics* **2003**, 22, 490. (c) Mitzel, N. W.; Losehand, U. *Angew. Chem.* **1997**, *109*, 2897. *Angew. Chem., Int. Ed. Engl.* **1997**, *36*, 2807. (d) Losehand, U.; Mitzel, N. W. *Inorg. Chem.* **1998**, *37*, 3175.
(9) Mitzel, N. W.; Losehand, U. *J. Am. Chem. Soc.* **1998**, *120*, 7320.
(10) Mitzel, N. W.; Losehand, U.; Wu, A.; Cremer, D.; Rankin, D. W. H. *J. Am. Chem. Soc.* **2000**, *122*, 4471.
(11) (a) Haszeldine, R. N.; Young, J. C. *J. Chem. Soc.* **1959**, 394. (b) Beckers, H.; Bürger, H. *J. Organomet. Chem.* **1990**, *385*, 207.
(12) *SHELXTL-PC 5.1*; Siemens Analytical X-ray Instruments Inc.: 1990.
(13) Huntley, C. M.; Laurenson, G. S.; Rankin, D. W. H. *J. Chem. Soc., Dalton Trans.* **1980**, 945.
(14) Fleischer, H.; Wann, D. A.; Hinchley, S. L.; Lewis, J. R.; Mawhorter, R. J.; Borisenko, K. B.; Robertson H. E.; Rankin, D. W. H. *J. Chem. Soc., Dalton Trans.*, in press.
(15) Hinchley, S. L.; Robertson, H. E.; Borisenko, K. B.; Turner, A. R.; Johnston, B. F.; Rankin, D. W. H.; Ahmadian, M.; Jones, J. N.; Cowley, A. H. *J. Chem. Soc., Dalton Trans.* **2004**, 2469.
(16) Ross, A. W.; Fink, M.; Hilderbrandt, R. *International Tables for X-ray Crystallography*; Wilson, A. J. C., Ed.; Kluwer Academic Publishers: Dodrecht, Boston, 1992; Vol. C., p 245.
(17) (a) Binkley, J. S.; Pople, J. A.; Hehre, W. J. *J. Am. Chem. Soc.* **1980**, *102*, 939. (b) Gordon, M. S.; Binkley, J. S.; Pople, J. A.; Pietro, W. J.; Hehre W. J. *J. Am. Chem. Soc.* **1982**, *104*, 2797. (c) Pietro, W. J.; Francl, M. M.; Hehre, W. J.; Defrees, D. J.; Pople, J. A.; Binkley J. S. *J. Am. Chem. Soc.* **1982**, *104*, 5039. (d) 6-31G(d): Hariharan, P. C.; Pople J. A. *Theor. Chim. Acta*, **1973**, *28*, 213. (e) Hariharan, P. C.; Pople, J. A. *Chem. Phys. Lett.* **1972**, *66*, 217. (f) 6-311G(d): Krishnan, R.; Frisch, M. J.; Pople, J. A. *Chem. Phys.* **1980**, *72*, 4244.
(18) Bader, R. W. F. *Atoms in Molecules: A Quantum Theory*; Clarendon Press: Oxford, U.K., 1990.
(19) (a) Carpenter J. E.; Weinhold, F. *THEOCHEM* **1988**, *169*, 41. (b) Reed, A. E. Weinhold, F. *J. Chem. Phys.* **1983**, *78*, 4066. (c) Reed, A. E.; Curtiss, L. A.; Weinhold, F. *Chem. Rev.* **1988**, *88*, 899.
(20) Frisch, M. J. et al. *Gaussian 98*, revision A.6; Gaussian, Inc.: Pittsburgh, PA, 1998.

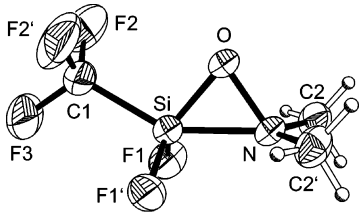

Figure 1. Molecular structure of $(F_3C)F_2SiONMe_2$ as determined by low-temperature X-ray diffraction

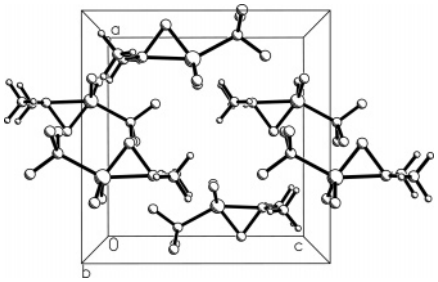

Figure 2. Packing diagram and unit cell of $(F_3C)F_2SiONMe_2$ as determined by low-temperature X-ray diffraction

at ambient temperature to give SiF_4 and an oily residue consisting of a complex mixture of CF_2 insertion products. Characterization had thus to be undertaken by gas-phase IR spectroscopy and by NMR spectroscopy in toluene solutions at −30 °C. In the ^{1}H, ^{13}C, ^{15}N, ^{19}F, and ^{29}Si NMR spectra signals with coupling patterns as expected (see Experimental Section).

In the $^{15}N\{^1H\}$ NMR spectrum one observes a triplet at −264.1 ppm, due to the long-range coupling $^3J_{NOSiF}$ (11.9 Hz) to the silicon-bound fluorine atoms. The chemical shift is 15 ppm lower in frequency than those of the related compounds $F_3SiONMe_2$ (−249.2 ppm) and $ClH_2SiONMe_2$ (−249.2 ppm). The ^{29}Si NMR shows a well resolved signal at −116.8 ppm split into a triplet ($^1J_{SiF}$ = 252.5 Hz) of quartets ($^2J_{SiCF}$ = 64.0 Hz).

Crystal Structure Determination. For the purpose of structure determination a single crystal of $(F_3C)F_2SiONMe_2$ was grown by in situ crystallization techniques at the melting point of −43 °C. X-ray diffraction gave the geometry depicted in Figure 1. The molecules in the crystal of $(F_3C)F_2SiONMe_2$ are nowhere closer than the sum of the respective van der Waals radii (see packing diagram in Figure 2). Thus the molecules in the crystal interact predominantly through "nonchemical" forces with a large probable contribution of their high molecular dipole moments.

The most intriguing structural findings describe the SiON skeleton and are the extremely acute SiON angle of 74.1° and the Si···N distance of 1.904 Å, which is shorter than the covalent Si−C bond to the CF_3 group (1.912 Å). This represents by far the strongest geminal Si···N interaction detected so far and leads to a coordination environment at silicon best described as trigonal bipyramidal (CF_3 and N axial, two F and O equatorial), distorted by the presence of the N−O bond. Consequently the latter is markedly widened as compared with standard values.

Gas Electron Diffraction. Earlier studies on SiON compounds[9,10] have revealed substantial dependence of the molecular structure on the polarity of the surrounding medium. The structure of the free molecule was therefore also determined by gas electron diffraction augmented by calculated values from the MP2/6-311G(d,p) level of theory, employing the SARACEN method for refinement.[22,23] The vapor of $(F_3C)F_2SiONMe_2$ consists of two conformers gauche and anti (Figure 3). The success of the refinement is obvious from the radial distribution curve shown in Figure 4.

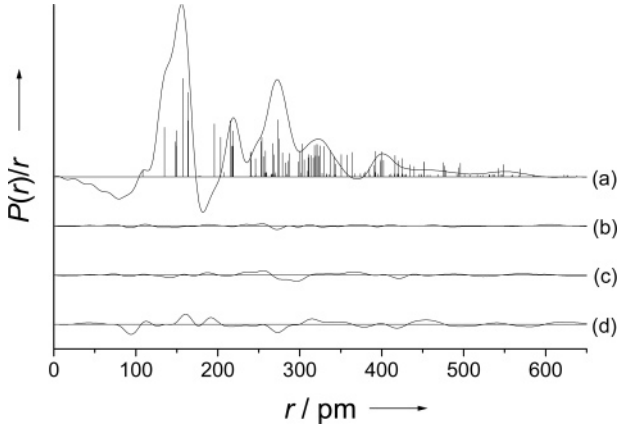

Figure 4. Experimental radial-distribution curve for $(F_3C)F_2SiONMe_2$ as determined by gas electron diffraction (a) and the difference curve (experimental−theoretical) (b) for a gauche:anti vapor composition of 60:40. Curves (c and d are the difference (experimental−theoretical) curves for the pure gauche and pure anti gas, respectively. Before Fourier inversion the data were multiplied by $s\cdot\exp(-0.000\,02s^2)/[(Z_{Si} - f_{Si})(Z_F - f_F)]$.

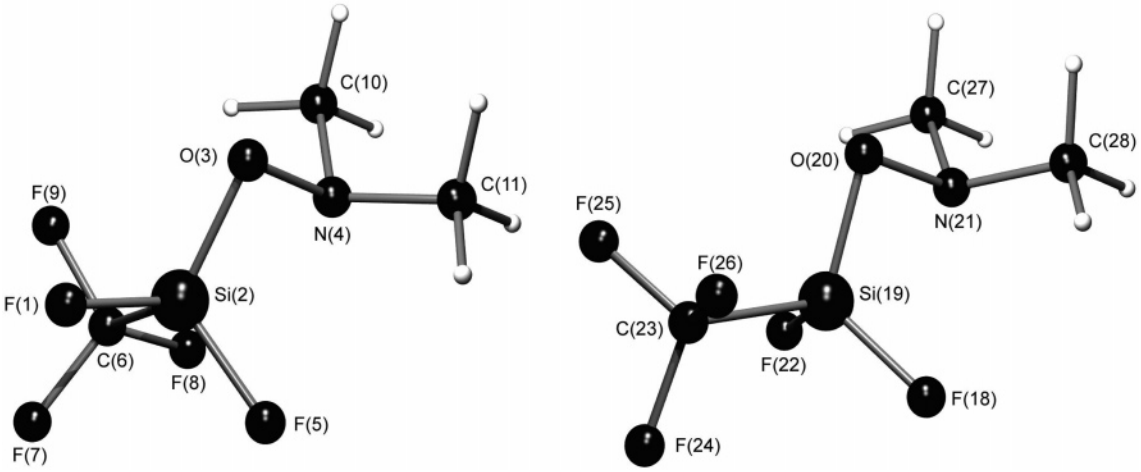

Figure 3. Molecular structures of the two conformers of $(F_3C)F_2SiONMe_2$ present in the gas phase as determined by gas electron diffraction: gauche (left picture), anti (right picture)

Table 1. Structural Parameters for the Two Conformers of $(F_3C)F_2SiONMe_2$ as Determined by Low-Temperature X-ray Diffraction (XRD), Gas Electron Diffraction (GED), and ab Initio Calculations at the MP2/6-311++G(d,p) Level of Theory (MP2)[a]

	anti conformer			gauche conformer	
parameter	XRD	GED	MP2	GED	MP2
*r*SiF	1.574(1)	1.577(3)	1.604[b]	1.578(3)	1.605[b]
*r*SiO	1.643(1)	1.640(7)	1.666	1.635(7)	1.661
*r*SiC	1.912(3)	1.956(8)	1.920	1.957(8)	1.922
*r*CF	1.315(4)^{ip} 1.346(2)^{oop}	1.350(2)	1.354[b]	1.349(2)	1.352[b]
*r*NO	1.515(2)	1.500(9)	1.488	1.497(8)	1.485
*r*NC	1.465(2)	1.482(6)	1.461	1.482(6)	1.462[b]
*r*Si···N	1.904(2)	2.112	2.059	2.174	2.097
∠ONC	108.5(1)	107.4(8)	107.3	107.4(8)	107.3[b]
∠SiON	74.1(1)	84.4(32)	81.3	87.8(20)	83.4
∠OSiC	99.8(1)	103.7(17)	103.0	119.4(12)	118.7
$\angle OSiF_{eq}$	120.6(1)	113.3(11)	117.3[b]	112.5(10)	115.5
$\angle OSiF_{ax}$				103.9(25)	104.7
∠SiCF	112.5(2)^{oop} 114.9(2)^{ip}	111.1(4)	112.0[b]	110.3(4)	112.0
$\angle F_{ax}SiON$				−180.1(22)	−176.8
$\angle F_{eq}SiON$[c]	72.5(1)	63.0(16)	67.9114.9(2)^{ip}	64.1(16)	69.0
∠CSiON	180.0	180.0	180.0	−64.7(41)	−63.7
∠SiONC[c]	118.3(1)	119.6(8)	119.7	119.6(8)	119.7
$\angle F_{ax}SiCF_{ax}$				73.0(25)	74.3
$\angle F_{ax}CSiO$	180.0	180.1(13)	180.0		

[a] ip: in plane. oop: out of plane. ax: Atom is in axial position. eq: Atom is in equatorial position. [b] Average value [c] Only the absolute value is considered.

The gauche conformer (double degeneracy) is the more abundant one with a contribution of 60%(±5%). This corresponds to a small difference in free energy between these conformers of only 0.7 kJ mol^{-1}, with the anti conformer being the ground state. The geometries of the two conformers are closely related (Table 1). Despite the similarity in electronegativities of F and the F_3C group, there is a substantial strengthening of the Si···N attractive force in both conformers [anti ∠SiON 84.4(32)°, gauche 87.8(20)°] relative to the compound $F_3SiONMe_2$ [∠SiON 94.3(9)°][9] for the free molecules in the gas phase. For $ClH_2SiONMe_2$[10] we have shown that the anti conformer [∠SiON 87.1(9)°] had a drastically stronger Si···N attraction than the gauche conformer [∠SiON 104.7(11)°], due to the electronegative substituent in the anti position relative to the N atom, the optimum orientation for a strong interaction of molecular group dipole moments. We expected a close similarity of the structures of the SiON fragments in $F_3SiONMe_2$ and in the gauche conformer of $(F_3C)F_2SiONMe_2$, as they have the same substituents in anti positions relative to the N atom. However, the difference between the gas-phase and solid-state geometries is much less pronounced in $(F_3C)F_2SiONMe_2$ than in $F_3SiONMe_2$[10] and $ClH_2SiONMe_2$[9] or other simple donor−acceptor adducts.[24] In contrast to the earlier investigations this demonstrates the predominant part of the Si···N attractive force to be of molecular origin and not due to interactions of the molecular dipole moments in the solid. The compound is thus a rare and important example of a volatile, intramolecularly hypercoordinate silicon compound[25] that can be investigated in the gas phase.

It should be noted that we observed extreme deviations between values calculated with different theoretical methods. The SiON angle of the anti conformer of $(F_3C)F_2SiONMe_2$ was predicted to be 114.0° at HF/6-311++G(d,p), 81.3° at MP2/6-311++G(d,p), 72.0° at MP2/TZV and 100.0° at B3PW91/6-311++G(d,p). These results show that correlated quantum mechanical methods are necessary to describe the Si···N interaction quantitatively. Hartree−Fock and DFT methods including a fraction of HF exchange underestimate the interaction, probably because there is a significant dispersive component. On one hand the results underline the importance of a proper high-level theoretical treatment of such systems, which are difficult to describe because of the shallow angle-bending potential; on the other hand they also underline the importance of accurate experimental structure determinations in the gas phase, as even when electron correlation is included, the results are highly dependent on the basis set chosen.

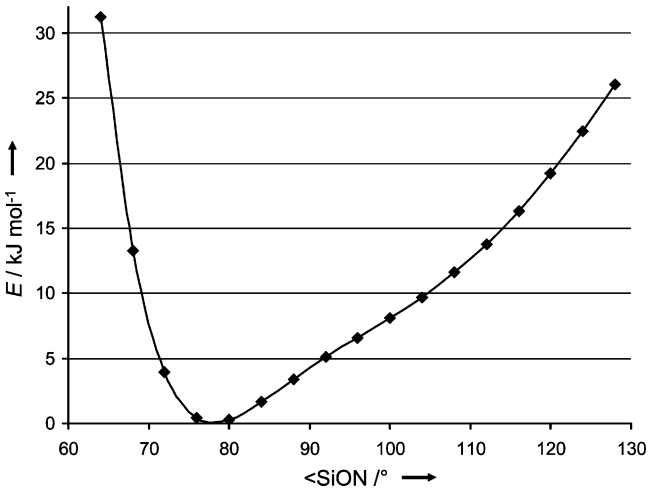

Figure 5. Potential curve for $(F_3C)F_2SiONMe_2$ as obtained by single-point energy calculations at the MP2-FC/6-311++G(3df,2p) level on geometries obtained by optimization at the MP2-FC/6-311+G(d) level with fixed SiON angles.

SiON Bending Potential. With the experimental methods of structural chemistry we could unequivocally show the existence of a force strongly distorting the coordination sphere at oxygen in $(F_3C)F_2SiONMe_2$. To get some information about the energetics of the systems we became interested in the bending potential of the SiON angle. The potential curve was calculated at the MP2/6-311++G(3df,2p)||MP2/6-311+G(d) level of theory (Figure 5). It shows a steep ascent on the low-angle side, while it is more flat for high angles. Besides the minimum at about 78° the curve has two points of inflection, which indicates that it is the result of different forces operative in the molecule. The general flatness of bending potentials at oxygen atoms bound to Si substituents is well established,[26] and combined with the steeper potential of the Si···N attractive interaction governed by electrostatic forces this could be a qualitative explanation for this unusual form of the potential curve. $(F_3C)F_2SiONMe_2$ is thus an exceptional case of a SiO compound with a strong contribution of a geminal attractive effect in all phases.

Atomic Charges. It is interesting to compare the dipole moments and atomic charges (Natural population analysis, NPA

(21) Biegler-König, F.; Schönbohm, J.; Bayles, D. AIM2000 − A Program to Analyze and Visualize Atoms in Molecules. *J. Comput. Chem.* **2001**, *22*, 545.
(22) (a) Blake, A. J.; Brain, P. T.; McNab, H.; Miller, J.; Morrison, C. A.; Parsons, S.; Rankin, D. W. H.; Robertson H. E.; Smart, B. A. *J. Phys. Chem.* **1996**, *100*, 12280. (b) Brain, P. T.; Morrison, C. A.; Parsons, S.; Rankin, D. W. H.; *J. Chem. Soc., Dalton Trans.* **1996**, 4589.
(23) Mitzel, N. W.; Rankin, D. W. H. *J. Chem. Soc., Dalton Trans.* **2003**, 3650.
(24) (a) Leopold, K. R.; Canagaratna, M.; Phillips, J. A. *Acc. Chem. Res.* **1997**, *30*, 57. (b) Jiao, H.; Schleyer, P. v. R. *J. Am. Chem. Soc.* **1994**, *116*, 7429.
(25) Akiba, K.-Y. *Chemistry of Hypervalent Compounds*; Wiley-VCH: New York, 1999.
(26) Schmidbaur, H. in *Tailor-made silicon−oxygen compounds*; Corriu, R., Jutzi, P., Eds.; Vieweg, Braunschweig, Germany, 1996.

Table 2. Calculated Atomic Charges (NPA Charges) for the Si, O, and N Atoms of $(F_3C)F_2SiONMe_2$ Dependent on the Valence Angle at Oxygen ∠SiON Obtained at the MP2/6-311++G(3df,2p)//MP2/6-311++G(d,p) Level of Theory[a]

∠SiON	68°	80°	92°	104°	116°	128°
Si	2.37	2.41	2.44	2.45	2.45	2.45
O	−0.72	−0.80	−0.84	−0.87	−0.89	−0.91
N	−0.44	−0.35	−0.30	−0.26	−0.23	−0.20
C(Si)	0.81	0.79	0.79	0.78	0.79	0.79
F(C)	−0.42	−0.42	−0.41	−0.41	−0.41	−0.41
F(Si)	−0.69	−0.68	−0.68	−0.68	−0.68	−0.68
C	−0.26	−0.26	−0.27	−0.27	−0.27	−0.28
H(av)	0.19	0.18	0.18	0.17	0.17	0.17

[a] Average values are given for the hydrogen atoms.

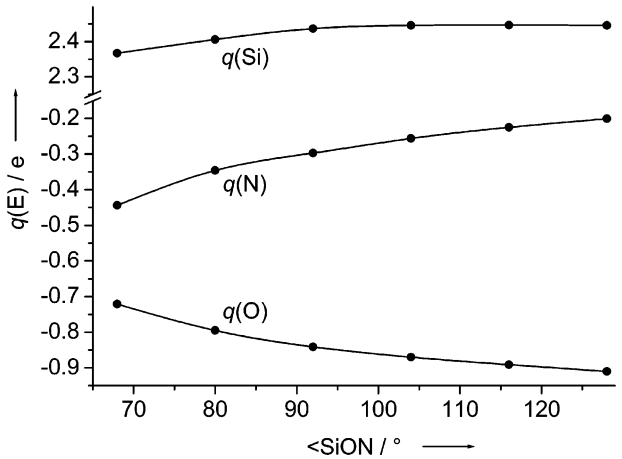

Figure 6. Calculated atomic charges (NPA charges) for the Si, O, and N atoms of $(F_3C)F_2SiONMe_2$ dependent on the valence angle at oxygen ∠SiON obtained at the MP2\6-311++G(3df,2p)//MP2/6-311+G(d,p) level of theory.

charges)[20] for the ground state and for a hypothetical molecule of $(F_3C)F_2SiONMe_2$ with the SiON angle fixed at 116°, which is approximately the structure expected for a molecule in the absence of an attractive Si···N interaction.[27] The charges are listed in Table 2, and the dependence of those of Si, O and N on the SiON angle is displayed in Figure 6. At some points charges were also calculated by integration of the electron densities over the atomic basins defined by AIM theory.[18] Although the absolute values are different for the two methods of calculation, the represented trends are the same, which adds to the reliability of the presented data. (Mulliken charges show a different trend but were excluded because they are of limited reliability.)

At the ground-state geometry and at ∠SiON = 116°, the dipole moments are 6.24 and 4.16 D, respectively. The corresponding charges on the Si atoms are 2.41 and 2.45 e and stay therefore almost unchanged upon formally switching the Si···N interaction on and off. In contrast, the charges at the N atoms are −0.35 and −0.23 e, respectively, which means that the N atoms become more negatively charged with increasing strength of the Si···N interaction in the three-membered ring. This is counterintuitive to the anticipated behavior of a classical dative bond, where charge is transferred from N to Si and is the case for normal donor−acceptor systems, even though in relatively small quantities for Si−N dative bonds.

It is also interesting to see that the negative charge on the O atom decreases with smaller SiON angles, meaning that the charge difference between the Si and O atoms decreases upon closing the SiON angle, thus leading to a less ionic contribution to Si−O bonding. This is surprising, as an extremely distorted coordination geometry at the O atom in the ground state of $(F_3C)F_2SiONMe_2$ could easier be realized with a more ionic Si−O bond with a low contribution of orbital directionality.

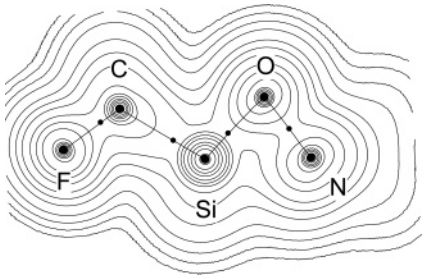

Figure 7. Calculated electron density map for $(F_3C)F_2SiONMe_2$ as obtained at the MP2/6-311++G(d,p) level of theory, showing bond critical points as solid dots (lines are printed at values of 0.002×10^n, 0.004×10^n, and 0.008×10^n e Å^{-1}, $n = 0, 1, 2, 3...$).

The increases of the molecular dipole moment and of the net charge separation between the Si and N atoms in the observed forms (Figure 5) suggest that the Si···N interaction is built up by transfer of electron density operative in a quite different way to that implied by the classical dative bond picture, as the gross electron density transfer is from the O to the N atoms (and to a smaller extent to the Si atoms).

Table 2 contains a summary of the data on atomic charges and also demonstrates that the charges on the SiON unit are most affected by the geometry changes, whereas the rest of the atoms retain their charges during the change of the SiON angle.

Topology of the Electron Density. The close proximity of the Si and N atoms and the clear presence of an attractive binding force between these geminal atoms suggest the existence of a bond-critical point in the topology of the electron density.[19] Figure 7 shows that this is clearly not the case. The absence of a bond critical point corresponds to a minimum of covalent contributions to this Si···N bond, resulting in the absence of charge density accumulation between these atoms. This is another indicator of the unsuitability of the classical picture of a dative bond[28] with a direct electron donation from nitrogen to silicon atoms.

The electron density parameters listed in Table 3 show the difference between the ground-state structure and a structure with the SiON angle fixed to 116°, which represents approximately the structure expected for a molecule without an operative Si···N attraction.[27] This comparison shows that the bonds to the silicon atom are charge-density depleted upon formation of the Si···N interaction. The most pronounced change occurs in the electron density of the Si−O bond at the bond critical point, which decreases by 7.3% upon Si···N bond formation. Such charge depleted bonds have also been observed for other hypercoordinate silicon compounds.[29] Upon formation of the Si···N bond the Si−O and N−O bonds become longer, in particular the latter. This is a further indication of ring formation.

The Laplacian of the electron density is shown in Figure 8. The typical features of a classical dative bond between Si and

(27) Mitzel, N. W.; Losehand, U.; Bauer, B. *Inorg. Chem.* **2000**, *39*, 1998.

(28) Haaland, A. *Angew. Chem.* **1989**, *101*, 1017; *Angew. Chem., Int. Ed. Engl.* **1989**, *28*, 992.

(29) Kocher, N.; Henn, J.; Gostevskii, B.; Kost, D.; Kalikhman, I.; Engels, B.; Stalke, D. *J. Am. Chem. Soc.* **2004**, *126*, 5563.

Table 3. Electron Density Topology Parameters for the Bonds in $(F_3C)F_2SiOMe_2$ in the Ground State and in a Structure with the SiON Angle Fixed to 116°, as Obtained at the MP2/6-311++G(d,p) Level of Theory[a]

	$(F_3C)F_2SiONMe_2$ ground state				$(F_3C)F_2SiONMe_2$ <SiON fixed to 116°			
A–B	*d*(A-bcp)	*d*(B-bcp)	$\rho(r_{bcp})$	$\nabla^2\rho(r_{bcp})$	*d*(A-bcp)	*d*(B-bcp)	$\rho(r_{bcp})$	$\nabla^2\rho(r_{bcp})$
Si−F	0.670	0.934	0.865	25.374	0.667	0.928	0.883	26.456
Si−O	0.674	0.992	0.882	20.983	0.664	0.966	0.951	24.188
Si−C	0.711	1.209	0.808	6.809	0.710	1.203	0.827	6.543
N−O	0.705	0.783	1.716	−1.905	0.668	0.792	1.791	−4.559

[a] The values given are the distances of the bond critical points (bcp) to the nuclear positions (in Å), the electron densities $\rho(r_{BCP})$ (in e Å^{-3}) at the bcp's, and the values of the Laplacians $\nabla^2\rho(r_{BCP})$ at the bcp's (in e Å^{-5}).

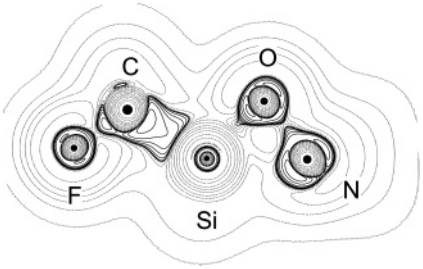

Figure 8. Calculated map of the Laplacian of electron density map for $(F_3C)F_2SiONMe_2$ as obtained at the MP2/6-311++G(d,p) level. (Lines are printed at values of 0.005×10^n, 0.01×10^n, and 0.02×10^n e Å^{-5}, n = 0, 1, 2, 3... Positive values are printed as red lines, and negative values as blue lines.)

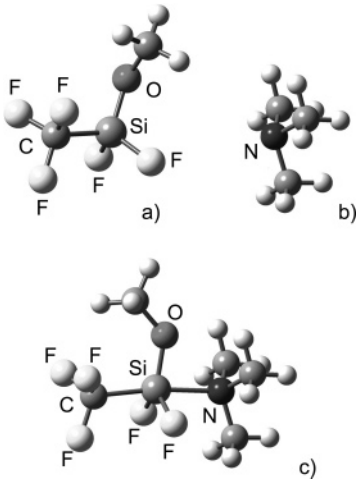

Figure 9. Molecular geometries of$(F_3C)F_2SiOMe$ (a), NMe_3 (b), and the adduct $(F_3C)F_2(MeO)Si{-}NMe_3$ (c) as obtained by MP2/6-31++G(d,p) calculations. Selected bond lengths [Å] and angles [deg] of the adduct (parameters of molecules a and b in parentheses): Si−N 2.069, Si−O 1.660 (1.609), Si−F 1.626/1.627 (1.589/1.598), N−C 1.448^{av} (1.455), N−Si−C 174.1, C−Si−O 111.5 (101.2), C−Si−F 91.8/91.9 (106.1/108.0).

N atoms are absent, but the charge concentration near the N atom representing the nitrogen lone pair of electrons is bent toward the attractor Si, which is charge-depleted. This topology will be discussed further in comparison to a typical dative bond below.

Comparison with an Open-Chain Silane−Amine Adduct with a Dative Bond. For comparison of the nonclassical bonding in $(F_3C)F_2SiONMe_2$ with closely related classically bonded systems, we have computed the optimized geometry and electronic properties of the adduct between the Lewis base NMe_3 (related to the NMe_2 group in $(F_3C)F_2SiONMe_2$) and the Lewis acid $(F_3C)F_2SiOMe$. This adduct has the same substitution pattern at silicon. The geometry of this adduct is shown in Figure 9 together with some important structural parameters in the figure caption.

Table 4. NPA Charges (e) of the Free Molecules of $(F_3C)F_2SiOMe$ and NMe_3 and of the Adduct $(F_3C)F_2(MeO)Si{-}NMe_3$ as Obtained by MP2/6-31++G(d,p) Calculations

	$(F_3C)F_2SiOMe$		NMe_3		
atom	in the adduct	in the free molecule	atom	in the adduct	in the free molecule
Si2	2.34	2.40	N1	−0.67	−0.60
O3	−1.03	−1.01	C9	−0.27	−0.26
C4	−0.10	−0.09	H10	0.20	0.17
H5	0.17	0.16	H11	0.20	0.17
H6	0.16	0.15	H12	0.16	0.13
H7	0.15	0.17	C13	−0.27	−0.26
C8	0.78	0.76	H14	0.20	0.17
F21	−0.69	−0.66	H15	0.20	0.17
F22	−0.69	−0.67	H16	0.16	0.13
*F*23	−0.44	−0.40	C17	−0.27	−0.26
F24	−0.43	−0.41	H18	0.20	0.17
F25	−0.41	−0.40	H19	0.20	0.17
			H20	0.16	0.14
sum	−0.18	0	sum	+0.18	0

The adduct formation energy was estimated by calculations based on geometries obtained at the MP2/6-311++G(d,p) level. NMe_3 and $(F_3C)F_2SiOMe$ were first optimized, and then their energies were compared to those with geometries adopted by these units in the adduct. The relative distortion energy is relatively small for NMe_3 (9.4 kJ mol^{-1}), but substantial for the $(F_3C)F_2SiOMe$ fragment, with 125.4 kJ mol^{-1}, corresponding to the change from a tetrahedral coordination geometry of the Si atom of $(F_3C)F_2SiOMe$ in the free molecule to trigonal bipyramidal in the adduct. The counterpoise corrected fragment energies were then compared to that of the adduct, which results in an energy difference of −171.5 kJ mol^{-1}. Overall these distortions and the bond formation energy give a total adduct formation energy of −36.7 kJ mol^{-1}, characterizing $(F_3C)F_2(MeO)Si{-}NMe_3$ as a relatively weakly bound adduct.

To test whether the adduct formation is accompanied by a transfer of electron density from the Lewis base to the Lewis acid, we calculated the atomic charges of all atoms from our highest level calculations by the NPA method. The results are shown in Table 4.

There is charge transfer in the adduct leading to a less positive charge on silicon and to a less negative charge on nitrogen in the adduct as compared to the free components. The peripheral atoms also participate in charge transfer: on one hand all the F atoms of the $(F_3C)F_2SiOMe$ unit become more negatively charged upon adduct formation, and on the other all H atoms of the NMe_3 unit get a more positive charge. In essence the sums of the NPA charges indicate that 0.18 elemental charges are transferred from NMe_3 onto the $(F_3C)F_2SiOMe$ unit in the adduct (comparing satisfactorily to the AIM charge transfer of 0.26 e). These values are of course far less than expected from

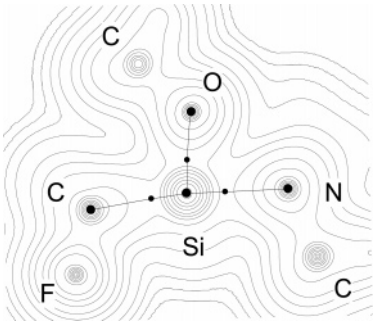

Figure 10. Calculated electron density map for $(F_3C)F_2(MeO)Si-NMe_3$ in the SiON plane as obtained at the MP2/6-311++G(d,p) level of theory, showing bond-critical points as solid dots. (Lines are printed at values of 0.002×10^n, 0.004×10^n, and 0.008×10^n e Å^{-1}, $n = 0, 1, 2, 3...$)

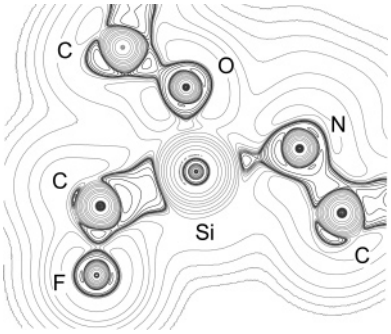

Figure 11. Calculated map of the Laplacian of electron density map for $(F_3C)F_2(MeO)Si-NMe_3$ in the SiON plane as obtained at the MP2/6-311++G(d,p) level. (Lines are printed at values of 0.005×10^n, 0.01×10^n, and 0.02×10^n e Å^{-5}, $n = 0, 1, 2, 3...$ Positive values are printed as red lines, and negative values as blue lines.)

the classical picture of the donation of an electron pair but are in accordance with earlier data for the $H_3N \rightarrow SiF_4$ adduct, which was intensely investigated experimentally by rotational spectroscopy[30] and theoretically in terms of the AIM method,[31] predicting a transfer of only 0.08 e in this case.

This was interpreted as a dominant contribution of electrostatic forces resulting from the change of the molecular dipole moment of zero in tetrahedral SiF_4 to a large value of 3.24 D for the distorted SiF_4 unit in its adduct geometry. The problem with this interpretation is, of course, that SiF_4 also forms a double adduct, $F_4Si(NH_3)_2$, in which the SiF_4 fragment is square planar and does not have a dipole moment, but the AIM theory interprets such interactions in a more detailed view of an interaction of the local charge concentration at the lone pair position of the NMe_3 unit with the local charge depletion at silicon,[22] which is increased upon the geometry change from tetrahedral to square-planar SiF_4 geometry and located above and below the SiF_4 plane in the adduct.

For the adduct $(F_3C)F_2(MeO)Si-NMe_3$ it was easy to locate a bond critical point between the Si and N atoms. These topology analyses were based on a wave function calculated at the MP2/6-311++G(d,p) level of theory. The electron density map and that of the corresponding Laplacian are shown in Figures 10 and 11, respectively. The Laplacian shows the high charge concentration at the N atom in $(F_3C)F_2(MeO)Si-NMe_3$ and the interaction with the charge depletion region at the Si atom.

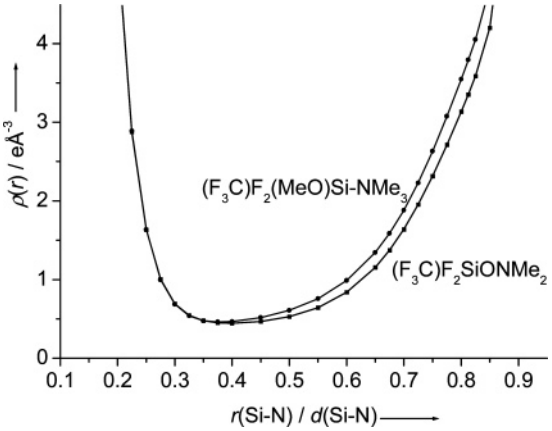

Figure 12. Electron density along the Si−N connecting lines in $(F_3C)F_2$-$SiONMe_2$ and $(F_3C)F_2(MeO)Si-NMe_3$ as calculated at the MP2/6-31++G-(d,p) level of theory. The units for the position are relative to the Si−N distances normalized to unity.

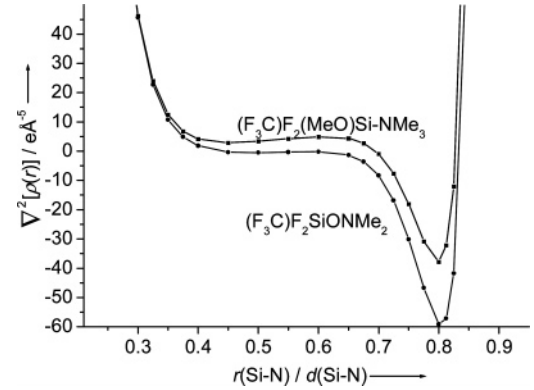

Figure 13. Laplacian of the electron density along the Si−N connecting line in $(F_3C)F_2SiONMe_2$ and $(F_3C)F_2(MeO)Si-NMe_3$ as calculated at the MP2/6-31++G(d,p) level. The units for the position are relative to the Si−N distances normalized to unity.

To get a more detailed view of the electronic situation in the region between Si and N atoms we calculated the electron density and the Laplacian values along the Si−N interaction path. These can be compared to the corresponding values in $(F_3C)F_2SiONMe_2$ along the Si−N connecting line (which is not a bond path according to the electron density topology in this case). The comparison of these values is best achieved graphically and shown in Figures 12 and 13. Note that the Si···N distances in the two molecules are slightly different, and therefore the figures refer to relative distances as fractions of the different Si−N distances.

The charge distributions between Si and N are surprisingly similar for the two molecules, and in particular at the silicon side they are almost identical. Only close to the nitrogen atom is there a slightly higher electron density in the adduct (F_3C)-$F_2(MeO)Si-NMe_3$ than in $(F_3C)F_2SiONMe_2$. This can be explained by the nitrogen lone pair being directly aligned in the Si−N direction, whereas in $(F_3C)F_2SiONMe_2$ it deviates from the Si−N vector. This becomes obvious from Figure 8, which shows the Laplacian of $(F_3C)F_2SiONMe_2$ in the SiON plane. The lone pair electron density is attracted toward the electron depletion region at silicon, but a complete alignment with the Si−N vector cannot be achieved.

The analysis of the Laplacian of the electron density along the Si−N lines in the two molecules also shows a high degree

(30) Ruoff, R. S.; Emilsson, T.; Iman, A. I.; Germann, T. C.; Gutowski, H. S. *J. Chem. Phys.* **1992**, *96*, 3441.
(31) Keith, T. A.; Bader, R. F. W. *J. Chem. Phys.* **1992**, *96*, 3447.

of similarity in their trends. The Laplacian of $(F_3C)F_2SiONMe_2$ adopts smaller values throughout the whole region than that of the adduct and is slightly negative in the middle of the SiN bond, whereas that of the adduct adopts positive values in this region. There is also a more pronounced local maximum of $\nabla^2\rho(r)$ at about 0.6 of the Si−N connecting line in the adduct, while the curve for $(F_3C)F_2SiONMe_2$ is almost flat in this region. At the point of smallest charge density (coincident with the bcp for the adduct) the Laplacian of both molecules is positive, which is generally observed for closed shell interactions (ionic bonds), as a result of the electron density being contracted to either nucleus of the interacting atoms.[33] It is interesting to note that the characteristics of these Laplacian distributions are very similar to those of a hexacoordinate silicon compound recently investigated by Stalke et al.,[29] indicating at least some degree of similarity of the nature of bonding in these systems.

Cremer and co-workers have introduced the use of the total energy density, $H(r)$, as a hallmark for the classification of bonds. It complements the Laplacian in the analysis of bond types and is defined as $H(r) = G(r) + V(r)$, where $G(r)$ and $V(r)$ represent the potential and kinetic energy densities, respectively.[33] The value of $H(r)$ at the bond critical point is negative for "shared interactions" and positive for "closed shell interactions" (ionic bonds). For the adduct $(F_3C)F_2(MeO)Si-NMe_3$ H(bcp) adopts a value of 0.105, classifying this bond as a closed shell interaction. At the point of lowest electron density on the Si−N vector in $(F_3C)F_2SiONMe_2$, $H(r)$ is 0.101 and thus again very similar to that of the adduct at its bcp.

Conclusion

$(F_3C)F_2SiONMe_2$ is a well suited model compound for an investigation of the nature of the bonding forces between Si and N atoms in geminal Si/N systems. Such kinds of interactions were first postulated as classical dative bonds between N and Si to explain a series of anomalies in physical properties and chemical behavior of α-aminosilanes. So far interactions between geminal Si and N atoms have been established unequivocally by different experimental methods for SiON and SiNN units, but not in a single case for the aminomethylsilanes (SiCN units) for which they were originally postulated.

$(F_3C)F_2SiONMe_2$ shows a very strong Si···N interaction, which leads to a Si···N distance shorter than the Si−C bond in the same molecule. Notwithstanding the clear three-membered ring structure of this molecule detected on the basis of X-ray diffraction of the crystalline substance and electron diffraction in the gas, the "molecular graph" derived from an analysis of the topology of the electron density represents an open chain molecule. Notably, the Si···N interaction is not recognized as a "bonding interaction" or an "atomic interaction line" in terms of the theory of atoms in molecules (AIM).[19] This is obviously due to the fact that the electron density on the connecting line between the Si and N atoms is very low, as is usual for dative bonds, such as in our reference molecule, the adduct $(F_3C)F_2(MeO)Si-NMe_3$. The close proximity of the Si···N interaction line to the electron density cloud belonging to the oxygen atom causes a superposition dominated by the electron density on oxygen, making a Si···N interaction difficult to detect by this method. This is obvious by comparison of the three principal curvatures, λ_1, λ_2, and λ_3, of $\rho(r)$ at the points of lowest electron density along the Si−N connecting lines [$(F_3C)F_2SiONMe_2$ λ_1 −0.066, λ_2 0.049, and λ_3 0.188; $(F_3C)F_2(MeO)Si-NMe_3$ λ_1 −0.073, λ_2 −0.071, and λ_3 0.316], leading to the detectability of a bond critical point for the $(F_3C)F_2(MeO)Si-NMe_3$ adduct. It should be noted that the absence of bond critical points in three-membered ring systems might not be restricted to $(F_3C)F_2SiONMe_2$ but may also be found in $(F_3C)_2BCH_2NMe_2$.[35] The latter has a three-membered BCN ring system with three angles close to 60°, which we will discuss in more detail in a forthcoming contribution.

The flat bending potential of $(F_3C)F_2SiONMe_2$ shows that the Si···N bond is a weak interaction, although it remains difficult to provide a reliable estimate for the interaction strength, as energy is gained by the Si···N interaction, while energy has to be afforded for overcoming the deformation of the coordination sphere of oxygen and the two effects are difficult to separate.

The lack of a bond-critical point between Si and N is indicative of the absence of a significant covalent contribution. The comparison of the atomic charges of the ground state of $(F_3C)F_2SiONMe_2$ with those of a structure with a SiON angle fixed to 116° (estimated structure without SiON interaction) shows that the typical charge transfer from a Lewis base to a Lewis acid upon adduct formation is not observed for this compound. In contrast, the N atom of $(F_3C)F_2SiONMe_2$ even accumulates negative charge upon formation of the Si···N bond and a three-membered SiON ring, while the O atom becomes more positively charged. This makes the interaction in $(F_3C)F_2SiONMe_2$ different from those in adducts such as $(F_3C)F_2(MeO)Si-NMe_3$ and justifies its description as a nonclassical bond.

The typical components for a dative bond, which are ionic interactions (including interaction of the dipole moments), charge transfer, small covalent contributions, and dispersive components, are found to be present in the adduct $(F_3C)F_2(MeO)Si-NMe_3$. The inability of $(F_3C)F_2SiONMe_2$ to align its nitrogen lone pair exactly toward the Lewis acidic Si center seems to prevent a covalent contribution. The presence of the additional attractor, oxygen, between the formal "base" and "acid" partners, N and Si, allows for rearrangement of electron density via this bridge and mainly between N and O atoms, so that a net charge transfer to silicon is avoided. However, the electrostatic attraction is increased by negative charge accumulation at the N atom.

The Si···N bond in $(F_3C)F_2SiONMe_2$ could thus be coarsely described as a dative bond with covalent and classical charge-transfer contributions switched off, while increasing the electrostatic component by increasing the negative charge on N.

The so-called α-effect must therefore be critically revisited, and it needs many more investigations on simple model systems with other donor, acceptor, and linker functions for the development of a more appropriate description of bonding in geminal systems, in particular for the industrially important α-silanes.

(32) Koritsanszky, T. S.; Coppens, P. *Chem. Rev.* **2001**, *101*, 1568.
(33) Jonas, V.; Frenking, G.; Reetz, M. T. *J. Am. Chem. Soc.* **1994**, *116*, 6, 8741.
(34) Cremer, D.; Kraka, E. *Angew. Chem., Int. Ed. Engl.* **1984**, *23*, 627.
(35) $(F_3C)_2BCH_2NMe_2$ is one of a series of known aminomethylboranes with three-membered BCN rings: (a) Brauer, D. J.; Bürger, H.; Buchheim-Spiegel, S.; Pawelke, G. *Eur. J. Inorg. Chem.* **1999**, 255. (b) Ansorge, A.; Brauer, D. J.; Bürger, H.; Hagen, T.; Pawelke, G. *Angew. Chem., Int. Ed. Engl.* **1993**, *32*, 384.

Acknowledgment. This work is dedicated to Professor Herbert Schumann Becker on the occasion of his 70th birthday. This work was supported by the Royal Society of Chemistry through a journal grant and by Fonds der Chemischen Industrie. We are grateful to Priv.-Doz. Dr. H. Beckers (Wuppertal, Germany) for a gift of F_3CSiF_3 and to Dr. S. L. Hinchley (Edinburgh, U.K.) for scanning films.

Supporting Information Available: Values of calculated and experimental gas electron diffraction parameters for both conformers of $(F_3C)F_2SiONMe_2$, a list of selected distances, amplitudes of vibration and k-values, a list of restraints on geometrical parameters and amplitudes used in the GED refinement, an experimental molecular-scattering intensity curve, Cartesian coordinates for all calculated molecules. This material is available free of charge via the Internet at http://pubs.acs.org.

JA052865O